Research Article

Chih-Yu Huang and Rongguang Liang*

Diamond turning fabrication of an ultra-compact endoscope

DOI 10.1515/aot-2016-0032
Received May 9, 2016; accepted June 29, 2016; previously published online July 21, 2016

Abstract: In this paper, we propose a technique by integrating mechanical mounts into lens elements to fulfill a self-aligned and self-assembled optical system. To prove this concept, we designed, fabricated, and tested an ultra-compact endoscope that adopts this technique. By taking advantages of the specially designed fixture and observing the interference fringes between the lens and fixture, we developed a method to minimize decenter and tilt between the two surfaces of the endoscope lens during the diamond turning fabrication process. The integrated mechanical mounts provide an easy assembly process for the endoscope system while maintaining high accuracy in system alignment. With the application of heat shrink tube as the endoscope system holder and to block stray light, the proposed endoscope system has the advantages of low cost, compact size, and high imaging quality.

Keywords: diamond turning fabrication; endoscope; optical system.

1 Introduction

Diamond turning is an ultra-precision fabrication method for generating spherical and freeform surfaces with submicrometric form accuracy and can reach surface roughness of only several nanometers. Besides, with the high resolution and straightness of the machine axes, we can also have a very accurate control of the other specifications of the lens such as lens thickness, lens diameter, lens decenter, and tilt. It is therefore advantageous to utilize these ultra-precision characteristics of the diamond turning machine to fabricate complex lens systems both for high imaging quality and for fast prototyping. There have been many publications about the diamond turning fabrication of freeform lenses or other complex lenses in all aspects of applications [1–8]. However, there are relatively few publications about the fabrication, alignment, and assembly process analysis of ultra-compact lenses [9–11]. In this paper, we propose a new technique in designing ultra-compact lens system that integrates mechanical mounts into each lens element. We can directly assemble the lenses without lens barrel for holding the lenses. This optical system is therefore very compact, lightweight, low cost, and easy to assemble while having high imaging quality. To demonstrate the concept, we designed and prototyped a three-lens endoscope system that adopts this technique. In this design, we used a complementary metal-oxide semiconductor (CMOS) sensor that is 400 pixels by 400 pixels with each pixel size of 3 μm by 3 μm. The size of the sensor array is therefore 1.2 mm by 1.2 mm, and the sensor dimension is 1.8 mm by 1.8 mm including packaging. As a result, we set the outer diameter of endoscope lenses to be 1.8 mm to match the size of the sensor. The design specifications are listed in Table 1, and the lens configuration of the proposed endoscope is shown in Figure 1. The endoscope has a diagonal half field of view of 27° and F/# of 4. Lens 1 and lens 3 are made from OKP-1, and lens 2 is made from polymethyl methacrylate (PMMA). OKP-1 is a flint-like material with low Abbe number (v=22) and high refractive index (n=1.64) (http://www.ogc.co.jp/e/products/fluorene/okp.html), while PMMA behaves like a crown material. With the combination of OKP-1 and PMMA, we can effectively correct chromatic aberration. Besides, both OKP-1 and PMMA are easy to fabricate through diamond turning process, and they are also suitable materials for plastic molding if mass production is desired in the future. Figure 2 shows the corresponding modulation transfer function (MTF). It shows that the endoscope has a diffraction-limited performance.

A tolerance analysis was performed in Zemax to verify that the endoscope could be fabricated in-house by the

***Corresponding author: Rongguang Liang,** College of Optical Sciences, University of Arizona, Tucson, AZ, USA, e-mail: rliang@optics.arizona.edu
Chih-Yu Huang: College of Optical Sciences, University of Arizona, Tucson, AZ, USA

Table 1: Design specifications of the proposed endoscope.

Diagonal half field of view	27°
F/#	4
Clear aperture	0.92 mm
Outer diameter	1.8 mm
Wavelength range	486–656 nm
Total length	3.469 mm

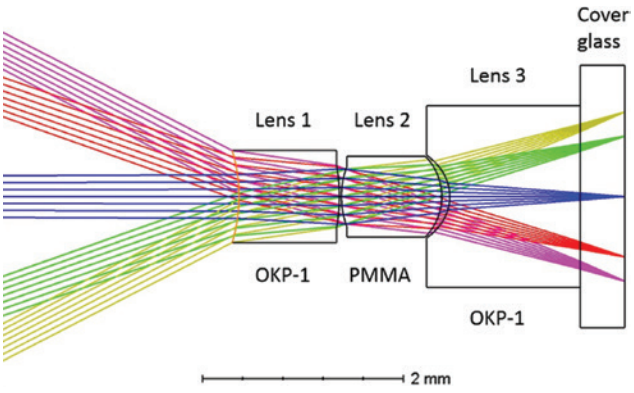

Figure 1: Lens configuration of the endoscope system.

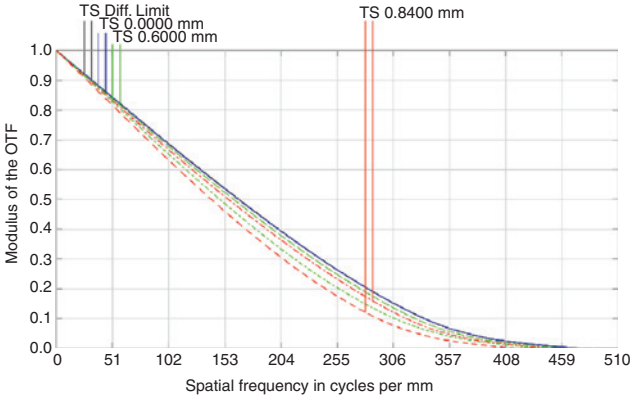

Figure 2: Modulation transfer function of the endoscope system.

diamond turning machine. The tolerances were set to have a worst case MTF of 30% at the Nyquist frequency, which is 166 cycles per millimeter at a test wavelength of 587 nm. As a comparison, the design has a nominal MTF of 45% at the Nyquist frequency. Table 2 lists the tolerance values based on the in-house diamond turning capability. A Monte Carlo simulation was performed to perturb the tolerance values listed in Table 2 and generate 500 samples. Over 90% of the Monte Carlo samples have the MTF of at least 33% at the Nyquist frequency. This simulation result shows that the proposed endoscope with adequate performance could be achieved in-house provided that the tolerance values in Table 2 are met.

Traditionally, lenses are assembled in the lens barrel with specially designed mechanical mounts that can both hold the lenses in place and help align each lens on the optical axis. However, the use of mechanical mount becomes challenging when the lens diameter reduces significantly to 2 mm or less. In such a case, not only is the fabrication of lens barrel and mechanical mounts extremely difficult but the finished lens barrel will also significantly increase the total size and weight of the system. The prototype we propose here integrates the mechanical mounts to the lens element itself so that we can simply clip each lens onto another lens element, and the mechanical mounts serve as the aligning and supporting purpose. As a result, there is no need to have an extra lens barrel to hold the lenses. Figure 3 shows the modified system layout from Figure 1 with the addition of mechanical mounts on each lens element, and Figure 4 shows the detailed dimensions of the mechanical mount in lens 1. From Figure 3, we can see that the clear aperture of each lens surface is unchanged, and the structures added onto the lens will not influence the imaging capability. In this

Table 2: Tolerance values for the proposed endoscope.

Radius of curvature (%)	±1
Thickness (μm)	±5
Surface decenter (μm)	±5
Surface tilt (°)	±0.1
Element decenter (μm)	±5
Element tilt (°)	±0.1
Index	±0.001
Abbe number	±1

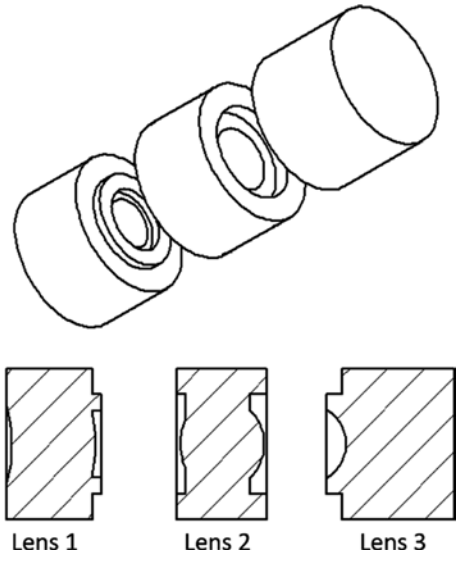

Figure 3: Modified endoscope system design considering integrated mechanical mounts.

modified design, we choose to have interference fit (press fit) between each neighboring lens element. This means that two parts are fastened together by friction after the parts are pushed together. As an example, the inner diameter of the mechanical mount at the left side of modified lens 2 is 1.2 mm, and in order to have the press fit for lenses 1 and 2, the outer diameter of the mechanical mount at the right side of modified lens 1 is set to be 1.19 mm. The same criterion is chosen for all the modified lens surfaces. Although there is a 12-μm air gap between lens 2 and lens 3 in the original design, this air gap can be maintained by the precise control of the thickness difference between the mechanical mounts on lens 2 and lens 3 during diamond turning process.

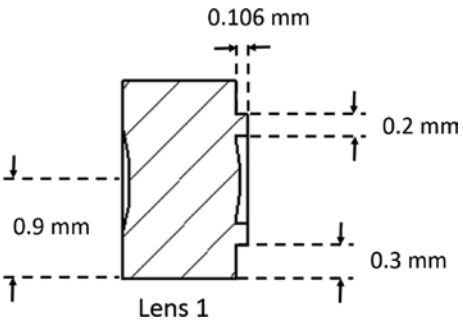

Figure 4: Detailed dimensions for the integrated mechanical mount on lens 1.

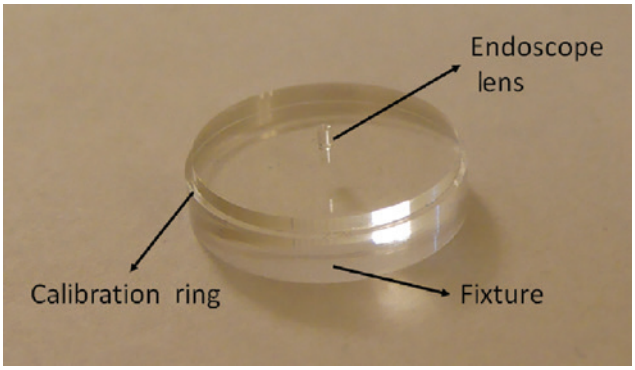

Figure 5: Fixture for ultra-compact lenses.

2 Alignment during fabrication process

One of the most important factors that will influence optical imaging quality of a diamond-turned optics is the misalignment between the two surfaces of the lens during fabrication process. In order to achieve high precision of the specifications for each lens in the proposed endoscope system, we investigated and developed some methods that can help to improve the alignment between lens surfaces. The misalignment can be divided into decenter and tilt. The decenter between the two surfaces of a lens is limited by the precision of the indication of each surface on the spindle center. For regular lenses, we can directly indicate each surface to be well-aligned on the spindle center whether the lens is fixed in the fixture or vacuumed on the spindle directly. However, this is usually not the case for ultra-compact lenses. The thickness for the lenses in this proposed endoscope system is no more than 1 mm, and once the lens is fixed into the fixture, there will be <0.5 mm of space for the indicator probe to contact the lens edge. As a result, it is challenging to directly indicate the lens.

Instead of directly indicating the lens itself, we cut another circular ring at the outer edge of the fixture for indication purpose during the fabrication process of the fixture so that this outer ring and the circular-step fixture structure are concentric at the spindle center. Figure 5 shows a detailed view of the fixture. Rather than indicating the lens, we can indicate the vertical side wall of the outer ring to make sure the fixture is centered at the spindle. By the precise control of the circular step size, we can be sure that the fixture can hold the lens strong enough and the displacement of the lens from the fixture center is kept within the tolerance specification. In our design, the step size of the fixture is set as 10 μm larger than the diameter of the lens. In this way, we can have a press fit between the lens and the fixture. Depending on the lens surface shape that is inserted into the fixture, we need to change the total number and the size of each circular step accordingly. As an example, Figure 6A shows the fixture for a lens with a concave surface. We only need to fabricate one step to properly hold the lens. On the other hand, Figure 6B shows the fixture for a lens with a convex surface. In this case, two steps are necessary. The first step is to hold the lens and fix it in the fixture center. The second step is only an open space to accommodate the convex surface and to avoid any contact between the fixture and the lens surface. According to our experiment, we can indicate the outer ring of the proposed fixture and align it on the spindle center with <0.2-μm radial runout. This means that most of the decenter of the lens comes from the displacement of the lens in the fixture circular-step structure, which is at most 5 μm in this case.

In order to verify the amount of displacement of the lens in the fixture circular-step structure, we cut a 3-mm long, 1.8 mm in diameter PMMA rod with the same cutting parameters as we fabricated the endoscope lenses. This PMMA rod was put into the fixture and glued. Then the

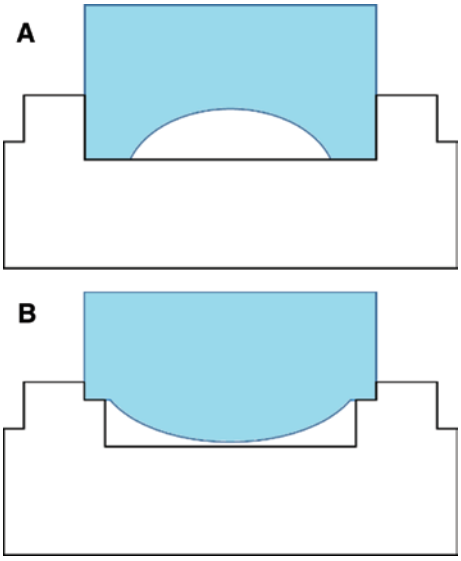

Figure 6: Modified fixture with an outer indication ring for (A) lens with flat or concave surface, or (B) lens with convex surface.

fixture was held on the spindle, and we indicated the outer ring of the fixture until we had about 0.2-μm radial runout, showing that the fixture was nicely centered on the spindle. Next we used the indicator to indicate the PMMA rod and read out the total radial runout value. This value corresponds to two times the decenter value between the PMMA rod and the spindle center. Figure 7 shows the setup of the experiment. This experiment procedure was repeated five times, and the mean value of the decenter was 1.53 μm with a standard deviation of 0.38 μm. The result shows that using the calibration ring on the fixture is effective, and the amount of decenter is within the tolerance listed in Table 2.

As for controlling the tilt between two surfaces of the lens element, we propose using interference fringes to minimize the tilt between the fixture front surface and the lens back surface, and it will in turn minimize the tilt between the two surfaces of the lens. We take the flat portion of the fixture surface that makes contact with the lens surface to be the reference flat. Depending on the fixture type we use, different flat surface on the fixture serves as the reference flat. As an example, in Figure 6A, the bottom surface of the central circular step is the reference flat, and in Figure 6B, the bottom surface of the smaller circular step that holds the convex surface serves as the reference flat. Once the lens is inserted into the fixture, the portion of the flat surface of the lens will have interference with the fixture flat surface provided that the wedge angle between these two surfaces is small enough. If the wedge angle is too large, there will be too many interference fringes present and therefore making the observation rather difficult. The working principle is similar to a Fizeau interferometer, but now the reference

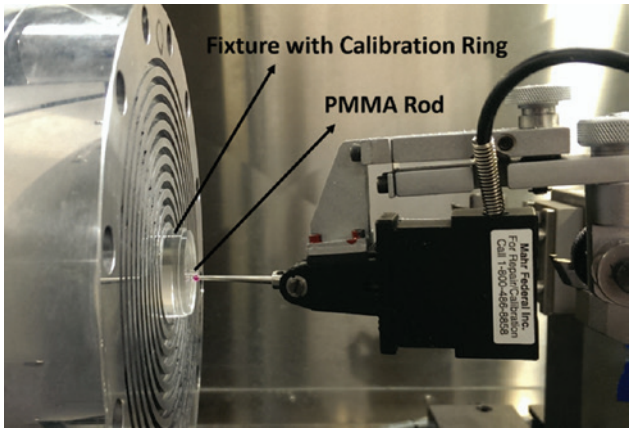

Figure 7: Setup for decenter measurement on the spindle.

surface is the fixture front flat surface and the test surface is the flat portion of the lens. Figure 8 shows some of the interferograms for a Fizeau interferometer [12]. By comparing the interferogram we acquire from the fixture and lens surfaces and the interferograms in Figure 8, we can easily have an understanding of how well the lens is aligned on the fixture. As the fixture surface and the lens surface are both flat, we would expect the interference fringes between these two surfaces to be straight lines. If the observed fringes are not straight, we know either the fixture flat surface or the flat surface of the lens is incorrectly fabricated, or there might be some deformation on the surfaces. By calculating the fringes, we can have a quantitative measurement on the amount of tilt. The quantitative calculation is out of scope of this paper. Figure 9 gives an example of the interference fringes between the fixture and one of the endoscope lenses. The lens surface that was in contact with the fixture is a flat surface. In this figure, we purposely created a small

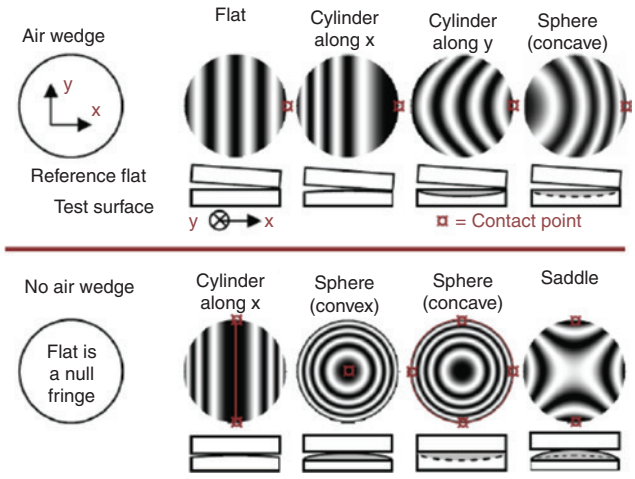

Figure 8: Some interferograms of Fizeau interferometer [12].

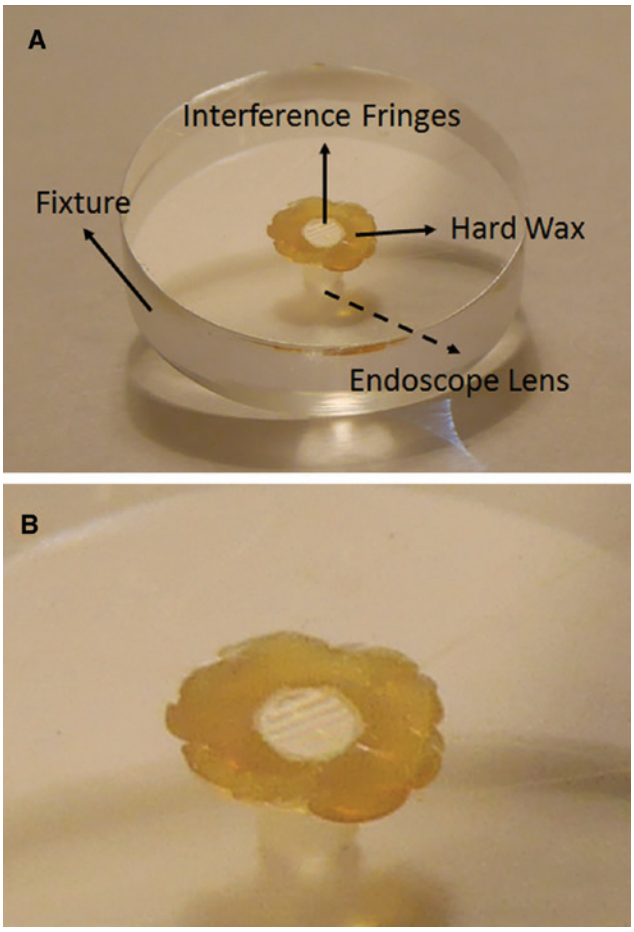

Figure 9: (A) The setup for observing interference fringes between the fixture and lens surface. (B) Enlarged interference fringes. We can clearly see the straight fringes, which means the two surfaces are flat, and there is no unexpected deformation. In order to minimize tilt, we need to null the fringes between these two surfaces.

amount of wedge between the lens and fixture surface to show the interference fringes.

All the fixtures we discussed so far were made from PMMA rod for low cost and fast prototyping. After the lens was put into the fixture, we used hard wax to secure them.

The tilt between the fixture and the lens surface is mainly caused by the difference between the internal diameter of the fixture and the diameter of the lens. Although this 10-µm difference in diameter is necessary for the lens to be press fitted into the fixture, it will inevitably cause tilt between the two surfaces if the lens is not perpendicularly inserted into the fixture. When there is tilt and the straight interference fringes are present, we can simply push one side of the lens surface and observe the motion of the fringes to know the direction of the wedge. We can then minimize the wedge by nulling the interference fringes. These procedures are done after we apply hard wax around the fixture and lens and before the hard wax is totally cooled down and hardened.

Before assembling the endoscope, we measure the tilt between the two surfaces of each lens to make sure they are within tolerances. We put a microscope slide under the Zygo NewView optical profilometer (Zygo Corp., Middlefield, CT, USA) and adjust the tilt of the stage to reduce the tilt of the microscope slide to 0.001°. We then put each lens on the microscope slide and measured the front surface. Next we removed tilt from the measurement result, and the amount we removed is the tilt between the front surface and the back surface of the lens. Figure 10A gives the tilt of lens 1, which is 0.023°. The tilt values for lens 2 and lens 3 are 0.052° and 0.064°, respectively. As a

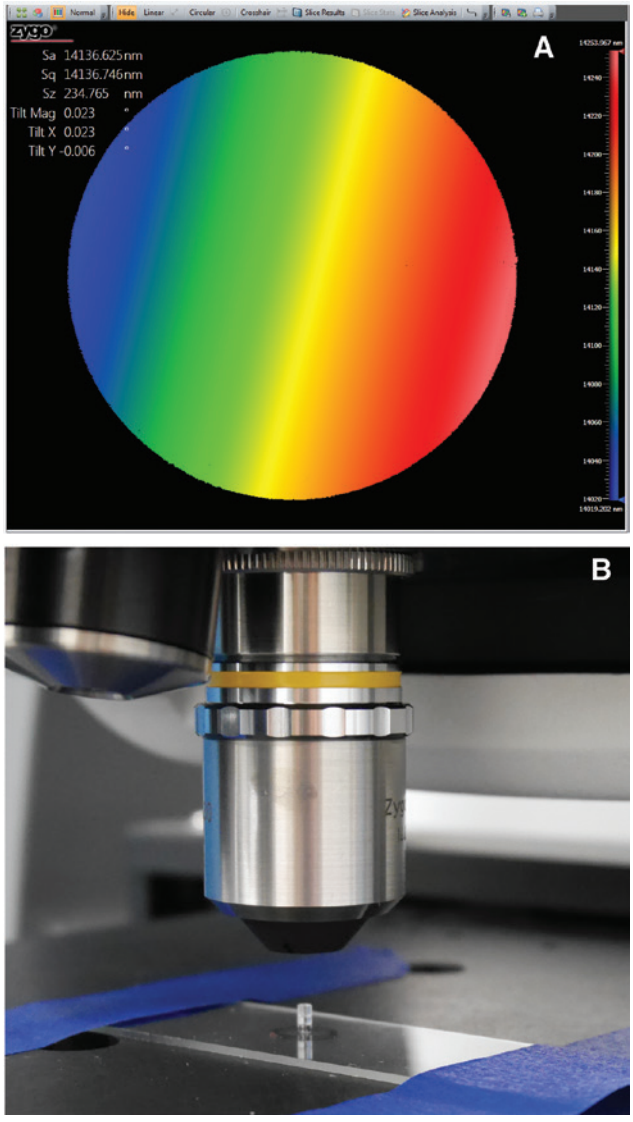

Figure 10: (A) Tilt measurement result for lens 1. (B) Setup for the tilt measurement for the whole endoscope system.

comparison, the tilt of the complete endoscope is 0.022°, and the setup is shown in Figure 10B. The result shows that the amount of tilt between the two surfaces is within the tolerance value listed in Table 2.

3 Assembly of the endoscope

Once we fabricate all three endoscope lenses, we can simply assemble them by pressing each lens and clipping onto another lens element to build the endoscope system. However, the resulting imaging quality was poor due to a large amount of stray light that went into the system from the outer structure of the lens element. Besides, although each lens can be clipped onto another, it is still not strong enough. In order to have a stable and reliable endoscope system, we need to do some extra steps in the assembly process. The first step is to blacken all the areas outside of lens clear aperture to minimize stray light that goes into the system. We use black ink and permanent marker to blacken these areas. For a compact system, this method is cost effective and time saving. After blackening the lenses and assembling the endoscope, we propose applying a heat shrink tube outside of the endoscope lenses as the supporting structure as well as a second layer to further reduce stray light. We chose a heat shrink tube with diameter slightly larger than that of the endoscope system, put the assembled three-lens endoscope into the heat shrink tube, used a micrometer to hold the endoscope lenses and heat shrink tube in place, and applied gentle heat to gradually shrink the heat shrink tube. Figure 11 shows the completed ultra-compact endoscope system after we attached the endoscope to the CMOS sensor. Here we applied a thin layer of polydimethylsiloxane (PDMS) to glue the endoscope onto the sensor cover glass to avoid any air gap between them. In Figure 11, we also show a complete set of individual endoscope lenses. The rightmost lens is blackened by a permanent marker to demonstrate how it can block stray light that comes from outside of field of view. Figure 12 shows a preliminary testing result of the endoscope system in resolving a 1951 USAF target. The smallest resolvable features are group 3, element 2 with a resolution limit of 8.98 line pairs per millimeter. The expected resolution limit is about 10.5 line pairs per millimeter. With this endoscope system, we can have a high resolution of the images. However, the contrast of the image is not as high as expected. One reason could be the limitation that we are not able to fully blacken the lens surface outside of the aperture stop. This causes a small amount of stray light going into the system from the mechanical mounts and eventually reaches the sensor. A more detailed study about the testing and stray light analysis of this endoscope system will be discussed in future work.

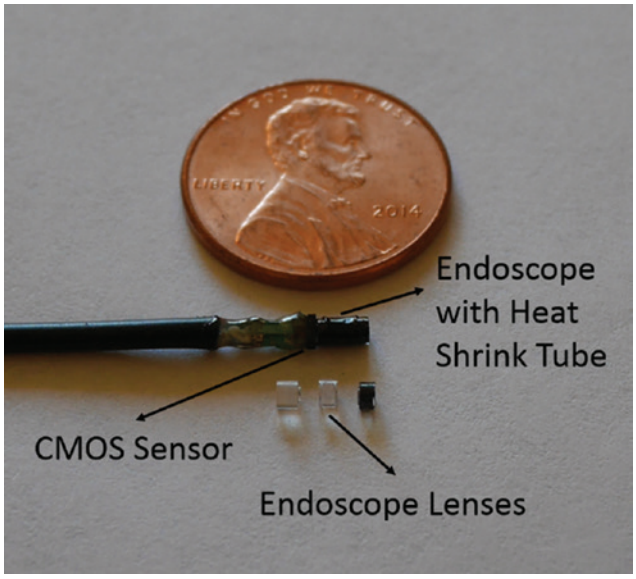

Figure 11: Proposed ultra-compact endoscope system.

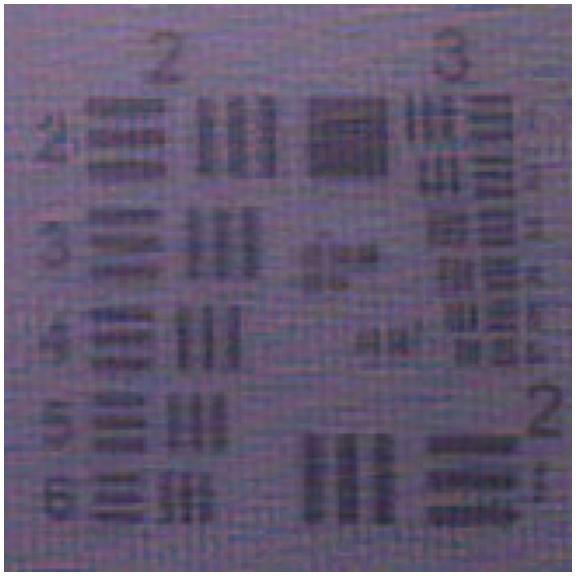

Figure 12: Preliminary testing result of the proposed endoscope system.

4 Conclusion

In this paper, we propose an ultra-compact endoscope system, which integrates the mechanical mounts into each lens element so that they can be assembled by simply clipping each lens into another. This configuration is therefore very compact, lightweight, easy to assemble, and low cost; it can maintain good imaging quality as well. To demonstrate

the concept, we designed and fabricated a three-lens endoscope system with the consideration of adding specific mechanical mount on each lens element. During the diamond turning fabrication process, we designed a fixture with an extra outer ring to help indicate the ultra-compact endoscope lens on the spindle center in order to minimize decenter between the two surfaces of the lens. We also used interference fringes to aid in correcting tilt between the lens and fixture. By observing the interference fringe patterns between the fixture flat surface and the flat portion of the lens surface and trying to null the interference fringes, we were able to minimize the tilt between the lens and the fixture, which in turn can significantly improve imaging quality of the lens system. Finally, we show the preliminary assembly and testing results of this endoscope system. By applying a heat shrink tube around the three-lens endoscope system, we can acquire a more solid system and further reduce stray light that goes into the system. A more detailed testing of the endoscope system as well as stray light analysis is under investigation. With proper modification of the lens design and mechanical mount structure, the size of the endoscope system can be further reduced to <1 mm.

References

[1] C. Huang, L. Li and A. Y. Yi, Microsyst Technol. 15, 4 (2009).
[2] S. To, T. C. Kwok, C. F. Cheung and W. B. Lee, In Proceedings of the SPIE (Vol. 6149, pp. 61490S) (2006).
[3] Z. Feng, B. D. Froese, C. Huang, D. Ma and R. Liang, Appl. Opt. 54, 20 (2015).
[4] H. Kim, K. Lee, K. Lee and Y. Bang, Int. J. Mach. Tools Manuf. 49, 12 (2009).
[5] L. Li and A. Y. Yi, Appl. Opt. 51, 12 (2012).
[6] R. Katkam, B. Banerjee, C. Y. Huang, X. Zhu, L. Ocampo, et al., J. Biomed. Opt. 20, 7 (2015).
[7] Z. Q. Yin, Y. F. Dai, S. Y. Li, C. L. Guan and G. P. Tie, Int. J. Mach. Tools Manuf. 51, 5 (2011).
[8] L. Li, A. Y. Yi, C. Huang, D. A. Grewell, A. Benatar, et al., Opt. Eng. 45, 11 (2006).
[9] M. Kyrish, J. Dobbs, S. Jain, X. Wang, D. Yu, et al., J. Biomed. Opt. 18, 9 (2013).
[10] R. T. Kester, T. Christenson, R. R. Kortum and T. S. Tkaczyk, Appl. Opt. 48, 18 (2009).
[11] F. C. Wippermann, E. Beckert, P. Dannberg, R. Eberhardt, A. Bräuer, et al., Proc. SPIE 7716, Micro-Optics (2010).
[12] E. P. Goodwin and J. C. Wyant, in 'Field Guide to Interferometric Optical Testing' (SPIE Press, Washington, 2006).